ENVIRONMENTAL RESEARCH
CLIMATE

PURPOSE-LED PUBLISHING™

Part of the ENVIRONMENTAL RESEARCH SERIES

PAPER • **OPEN ACCESS**

A new phase of land–atmosphere interactions in the East Asian Jet variability during summer

To cite this article: Jiyun Nam *et al* 2025 *Environ. Res.: Climate* **4** 045010

ENVIRONMENTAL RESEARCH
CLIMATE

Check for updates

OPEN ACCESS

RECEIVED
28 July 2025

REVISED
21 September 2025

ACCEPTED FOR PUBLICATION
7 October 2025

PUBLISHED
28 October 2025

PAPER

A new phase of land–atmosphere interactions in the East Asian Jet variability during summer

Jiyun Nam[1], Shih-Yu Simon Wang[2], Jee-Hoon Jeong[3], Hyungjun Kim[4] and Jin-Ho Yoon[1,*]

[1] School of Environment and Energy Engineering, Gwangju Institute of Science and Technology, Gwangju, Republic of Korea
[2] Department of Agronomy, Kasetsart University, Bangkok, Thailand
[3] Department of Environment and Energy, Center for Earth and Environment Research, Sejong University, Seoul, Republic of Korea
[4] Moon Soul Graduate School of Future Strategy, Korea Advanced Institute of Science and Technology, Daejeon, Republic of Korea
[*] Author to whom any correspondence should be addressed.

E-mail: yjinho@gist.ac.kr

Keywords: East Asian summer monsoon, East Asian Jet, regime shift, land–atmosphere coupling

Supplementary material for this article is available online

Abstract

The East Asian Jet (EAJ), a key upper-level westerly wind that controls monsoon circulation and precipitation patterns within the East Asian summer monsoon system, has undergone multiple regime shifts since the mid-20th century. While transitions in the late-1970s and mid-1990s are well documented, a more recent shift in the early 2000s remains less well characterized. Here we identify a regime shift of the EAJ occurring in 2002/2003 through striking changes, manifested by an abrupt intensification in both the mean state and interannual variance of the jet. This shift coincides with significant surface warming over southern China and widespread drying across East Asia. Our analysis identifies two key features characterizing this transition: strengthening of the Tibetan Plateau High (TPH) and emergence of enhanced SM–T coupling variability over Inner East Asia. After 2003, coupling strength exhibits significant correlation with surface energy partitioning and lower-tropospheric thermal structure. This coupling variability is closely linked to jet fluctuations, indicating that enhanced jet variability is strongly mediated by land–atmosphere (L–A) coupling processes. In addition, the intensified TPH additionally contributes to jet intensification through modifications in upper-tropospheric circulation patterns. These results highlight the critical role of L–A interactions in EAJ variability and provide insights into potential linkages between drought conditions under global warming and monsoon circulation changes mediated through upper-level atmospheric flow.

1. Introduction

The East Asian summer monsoon (EASM) represents one of the most important and dynamic climate systems on Earth, exhibiting variability across multiple timescales from interannual to multidecadal scales and exerting profound impacts on regional ecosystems, agricultural productivity, and extreme weather events across densely populated regions of East Asia (Huang *et al* 2007, Tao *et al* 2014, Lee *et al* 2017). Of particular scientific and societal importance are decadal transitions within the EASM system, often referred to as regime shifts, which represent fundamental reorganizations of monsoon circulation and associated precipitation patterns. These regime shifts have been extensively documented, with major transitions identified in the late 1970s (Lieting and Renguang 2000, Ding *et al* 2009, Zhou *et al* 2009, Ding *et al* 2010, Huang *et al* 2010, Tao *et al* 2014) and mid-1990s (Kwon *et al* 2005, Yim *et al* 2008, Ding *et al* 2009, Wu *et al* 2010, Chang *et al* 2014; Chen and Lu 2014, Dong *et al* 2016), characterized by strengthening and weakening of monsoon circulation and shifts in precipitation patterns.

Several studies have identified major EASM regime shifts through detailed analysis of the East Asian Jet (EAJ), which plays a crucial role in shaping the EASM system (Kwon *et al* 2007, Lu *et al* 2011, Lin *et al* 2024). The EAJ, characterized as a strong upper-level westerly wind system, fundamentally controls monsoon circulation patterns and determines the spatial and temporal distribution of rainfall across East Asia (Zhang *et al* 2006, Sampe and Xie 2010, Ha *et al* 2012, Wang *et al* 2013, Herzschuh *et al* 2019). Previous research by Kwon *et al* (2007) demonstrated that the EAJ underwent significant regime shifts in the late 1970s and mid-1990s, strongly linked to substantial changes in precipitation patterns over southern China through barotropic responses of upper tropospheric circulation.

Building upon this foundation, our analysis identifies an additional and previously underexamined regime shift in the EAJ occurring in 2002/2003, which serves as the primary focus of this study. While Lin *et al* (2024) recently reported a sharp increase in EAJ interannual variability since the late 20th century, attributing this change primarily to Atlantic Ocean forcing mechanisms, their analysis focused exclusively on remote oceanic teleconnections without examining the potential role of regional land–atmosphere (L–A) interactions in driving or modulating this enhanced variability.

Our investigation addresses this knowledge gap by exploring the concurrent emergence of enhanced soil moisture-temperature (SM–T)coupling over Inner East Asia and its relationship with EAJ variability changes during the post-2003 period. This research focus is motivated by well-documented observations of substantial soil moisture decline across East Asia during the same period (Rodell *et al* 2018, Scanlon *et al* 2018, Zhang *et al* 2020). While land surface conditions have traditionally been viewed as passive responses to atmospheric forcing, recent numerical studies suggest that soil moisture anomalies can affect upper-tropospheric circulation patterns through various physical mechanisms (Koster *et al* 2016, Martius *et al* 2021, Shi *et al* 2021b). However, robust observation evidence for such connections remains limited. Therefore, our study investigates whether regional L–A coupling is associated with enhanced EAJ variability, complementing the established oceanic forcing mechanisms. This perspective examines potential relationships between land surface conditions and jet behavior, providing insights into regional predictability mechanisms not captured by analyses focused solely on remote ocean forcing.

We address two main objectives in this study: (1) characterizing changes in EAJ mean state and variance during the recent period, focusing on the timing, magnitude, and spatial characteristics of these changes; (2) investigating the emergence of enhanced L–A coupling variability over East Asia and its relationship with EAJ behavior changes after 2003; and (3) examining the physical mechanisms that may link land surface conditions to upper-level circulation patterns through thermodynamic processes.

2. Methods

2.1. Data

We utilize various atmospheric and land surface variables from multiple reanalysis datasets. ERA5 (Hersbach *et al* 2019) provides monthly zonal wind (U), geopotential height (Z), and air temperature (T) at each of 37 pressure levels from 1958 to 2020, with a spatial resolution of $0.25° \times 0.25°$. Our analysis focuses on the boreal summer (JJA). Lower-tropospheric thickness is calculated from geopotential height differences between 500 and 1000 hPa to examine thermal structure changes in the lower atmosphere. To validate the robustness of regime shifts, we additionally use zonal wind data from JRA-55 (Kobayashi *et al* 2015; $1.25° \times 1.25°$) and 20CRv3 (Slivinski *et al* 2019, $1.0° \times 1.0°$).

Land surface variables, including 2 m air temperature, soil moisture, surface heat fluxes, and net radiation, are obtained from ERA5-Land (Muñoz-Sabater *et al* 2021, $0.1° \times 0.1°$). Surface heat fluxes follow the ERA5 convention where positive values indicate downward (toward surface) direction and negative values indicate upward (away from surface) direction. Volumetric soil moisture is obtained by integrating data from all four layers provided by ERA5-Land: 0–7 cm, 7–28 cm, 28–100 cm, 100–289 cm, yielding total column soil moisture from 0–289 cm depth. The whole-column approach is adopted to comprehensively assess regime shifts impacts on the full L–A interaction, as our analysis examines not only SM–T coupling but also the broader changes in surface energy partitioning including sensible heat flux, latent heat flux and their relationship to deeper soil moisture variations. The Bowen ratio (sensible/latent heat flux ratio) is also calculated to provide additional context for energy partitioning regimes.

Monthly precipitation data are from the GPCPv2.3 dataset (Adler *et al* 2003; $2.5° \times 2.5°$), covering 1979–2020. To verify the robustness of precipitation changes, we additionally analyzed two high-resolution gauge-based datasets: CPC Unified Gauge-Based Analysis of Daily Precipitation (Chen *et al* 2008, $0.5° \times 0.5°$) covering 1979–2020, and APHRODITE-I (Yatagai *et al* 2012, $0.25° \times 0.25°$) covering 1951–2015. These datasets allow us to confirm the robustness of precipitation variability across different spatial resolution and data sources. Sea surface temperature (SST) data are obtained from the Extended Reconstructed Sea Surface Temperature version 5 (ERSSTv5) dataset (Huang *et al* 2017a; $2° \times 2°$).

2.2. Change-point detection algorithm

To identify regime shifts in the EAJ variability, we apply three different change point detection algorithms to the EAJ index (EAJI) time series: (1) window-based change point detection, (2) cumulative sum (CUSUM), and (3) Binary Segmentation.

The window-based change point detection algorithm (Truong *et al* 2020) is designed to detect changes in statistical properties of a time series. The key advantage of this method is its ability to identify multiple change points in a single time series without a prior knowledge of the number or location of the change points. The algorithm uses a sliding window approach, moving a fixed-size window along the time series and comparing statistical properties within each window. In this study, we set the window size to 17 years and focus on detecting decadal-scale mean changes. Statistical significance is assessed through a bootstrapping procedure, with change points significant when $p < 0.05$.

Additionally, we employ the CUSUM algorithm (Page 1954), which identifies shifts by accumulating deviations from the mean over time. The strength of the CUSUM method lies in its sensitivity to detecting relatively subtle mean shifts without relying heavily on window size or prior assumptions of change point locations. The Binary Segmentation algorithm (Scott and Knott 1974) is also utilized, which iteratively partitions the data to identify multiple change points by detecting significant deviations in the mean or variance. This method is efficient in detecting abrupt shifts and is widely used due to its simplicity and computational effectiveness. For this study, we calibrate both algorithms to detect three mean-state change points.

2.3. Streamfunction budget analysis

Maintenance of upper-tropospheric stationary eddies were diagnosed using and streamfunction budget (Chen and Chen 1990). Let any field A be decomposed into a seasonal mean $\bar{A}$ and anomaly(transient) $A' = A - \bar{A}$. The subscript 'e' indicates the eddy component. Then, the streamfunction tendency ($\frac{\partial \bar{\psi}_e}{\partial t}$) at pressure level p is written as

$$\frac{\partial \bar{\psi}_e}{\partial t} = \nabla^{-2}\left[-\bar{\boldsymbol{V}}_\phi \cdot \boldsymbol{\nabla}\left(f+\bar{\zeta}\right)\right]_e + \nabla^{-2}\left\{-\boldsymbol{\nabla}\cdot\left[\bar{\boldsymbol{V}}_\chi\left(f+\bar{\zeta}\right)\right]_e\right\} + \nabla^{-2}\left\{-\boldsymbol{\nabla}\cdot\left(\overline{\boldsymbol{V}'\zeta'}\right)_e\right\} \approx 0.$$

Here, the first term of right-hand side is absolute vorticity advection by the rotational wind ($\bar{\boldsymbol{V}}_\phi$), the second term is divergence of absolute vorticity flux by the divergent wind ($\bar{\boldsymbol{V}}_\chi$), and the third term represents transient eddy vorticity fluxes. For the maintenance of stationary wave, the total sum of these three terms close to zero.

This diagnostic is used for separation of the dynamical roles that are otherwise entangled in geopotential or wind fields. Divergence term ($\nabla^{-2}\left\{-\boldsymbol{\nabla}\cdot\left[\bar{\boldsymbol{V}}_\chi\left(f+\bar{\zeta}\right)\right]_e\right\}$) quantifies remote forcing by divergence induced by diabatic heating, such as tropical convection, whereas advection term ($\nabla^{-2}\left[-\bar{\boldsymbol{V}}_\phi \cdot \boldsymbol{\nabla}\left(f+\bar{\zeta}\right)\right]_e$) captures local rotational redistribution/propagation that often damps the ridge near its core. Transient term ($\nabla^{-2}\left\{-\boldsymbol{\nabla}\cdot\left(\overline{\boldsymbol{V}'\zeta'}\right)_e\right\}$) is small for seasonal means and is therefore neglected in our analysis. The resulting quadrature (out-of-phase) relation between streamfunction and the two leading terms provides a mechanistic understanding for stationary wave maintenance—identifying where energy is supplied or sunk (divergence term) versus adjusted or propagated (advection term).

2.4. SM–T coupling strength

To quantify the strength of L–A coupling, we adopt the approach proposed by Miralles *et al* (2012), which assesses the coupling strength through the covariance between near-surface air temperature anomalies and the degree of soil moisture deficits. This metric is calculated as the product of the daily anomalies in near-surface air temperature (T') and the change in surface energy balance depending on the degree of soil moisture deficits (e').

The coupling strength (π) is calculated as follows:

$$\pi = T' * e' = T' * \left((R_n - \lambda E)' - \left(R_n - \lambda E_p\right)'\right).$$

In this formulation, R_n refers to the surface net radiation λE is the latent heat flux, and λE_p is the latent heat flux based on potential evaporation (E_p) instead of actual evaporation (E). The term e' becomes zero when soil moisture is sufficient to meet the atmospheric demand for evaporation, but increases under dry conditions as the atmospheric demand escalates. The anomalies are expressed as the number of standard deviations relative to the multiyear climatological mean for each day of the year.

This formulation effectively captures how soil moisture deficits redirect available energy from latent heat (evapotranspiration) to sensible heat flux, thereby influencing near-surface air temperature.

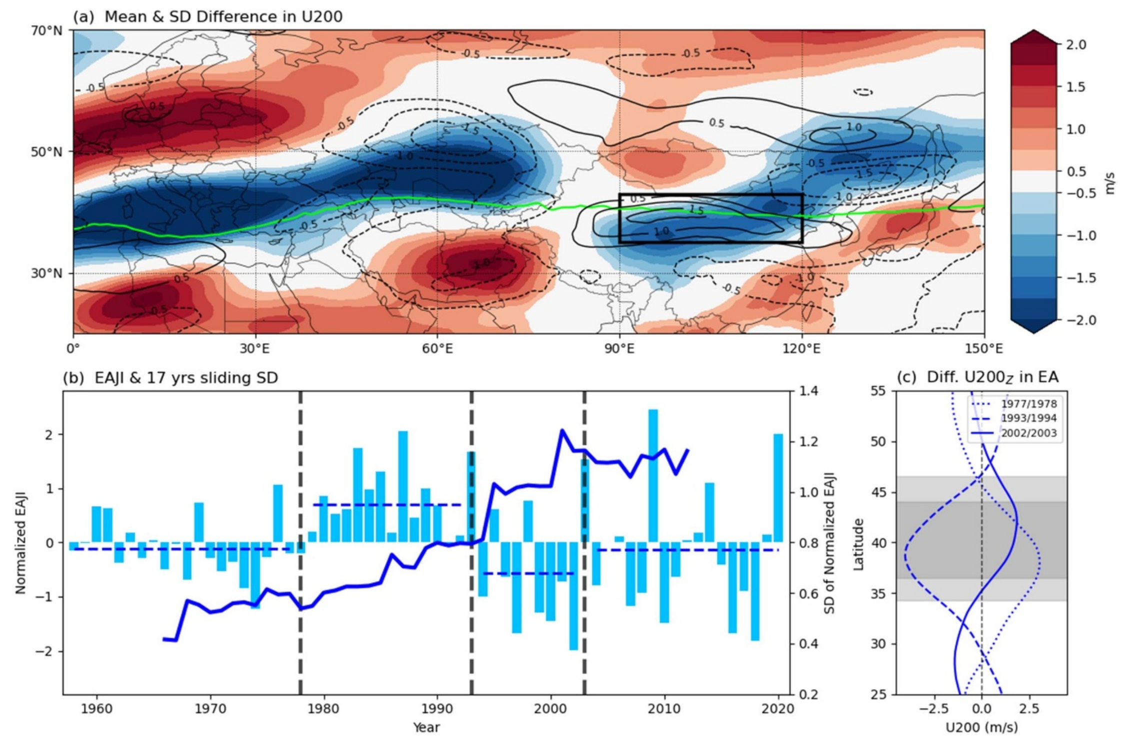

Figure 1. East Asian Jet Index (EAJI) and regime shift detection. (a) The mean difference (shaded) and the standard deviation difference (contour) of zonal wind at 200 hPa level (U200) between the past and the recent 30 years (1958–1987 minus 1991–2020). The green line indicates the location of the jet axis. Black box covers where we defined as the East Asian Jet region (90°–120° E, 35°–43° N). (b) Bars indicate the timeseries of the EAJI and blue line indicates its sliding standard deviation with 17 years window. The vertical dashed lines show the regime shift detected by the window-based change point detection algorithm and the horizontal dashed lines indicates the mean value of each sub-period. (c) Blue lines indicate the meridional displacement of jet during each regime shift, respectively. It is calculated by the difference of U200 zonal average ($U200_z$) over East Asian longitude band (90°–120 °E) during 1977/1978 shift (1965–1977 minus 1978–1992; dotted line), 1992/1993 shift (1978–1992 minus 1993–2002; dashed line), and 2002/2003 shift (1993–2002 minus 2003–2020; solid line). Light gray and dark gray shading show the ranges of $U200_z$ climatology which exceed 20 and 25 m s^{-1}.

Values of π less than or equal to zero indicate no coupling, while higher values indicate stronger coupling between available soil moisture and atmospheric temperature responses. To calculate the coupling strength, we first obtain daily-scale values and then aggregate to seasonal-scale values by averaging over the JJA period.

3. Results

3.1. The notable 2002/2003 EASM regime shift

We define the EAJI as area-averaged zonal wind at 200 hPa over the EAJ region (90–120° E, 35–43° N), representing the jet exit area downstream of the climatological Asian subtropical jet (Zhang *et al* 2006; figure 1(a)). Our region selection is based on robust multidecadal changes observed in both the mean state and standard deviation of the EAJ between 1958–1987 and 1991–2020 periods. The definition is also consistent with EAJ regions used in previous studies (Kwon *et al* 2007, Lin *et al* 2024), where the most pronounced changes in jet variability characteristics have been documented.

Application of window-based change point detection (see 'Methods') to the EAJI time series reveals significant regime shifts occurring in 1977/1978, 1992/1993, and 2002/2003 (figure 1(b)). These transitions demonstrate a consistent pattern of interdecadal changes in jet dynamics. The interdecadal mean of the EAJ increased substantially after 1978, decreased after 1993, and increase again after 2003. This temporal evolution reflects the complex interplay of multiple factors influencing East Asian atmospheric circulation, including both regional processes and remote teleconnections (Kim *et al* 2010, Ha *et al* 2012, Lee *et al* 2017).

Beyond these mean state transitions, the 17 year sliding stand deviation of the EAJI reveals a particularly striking feature (figure 1(b)). It shows a persistent and systematic increasing trend throughout the analysis period. An especially sharp and pronounced rise occurs in the early 2000s (figure 1(b)). This indicates a fundamental change in the nature of EAJ variability. The jet has become increasing unstable

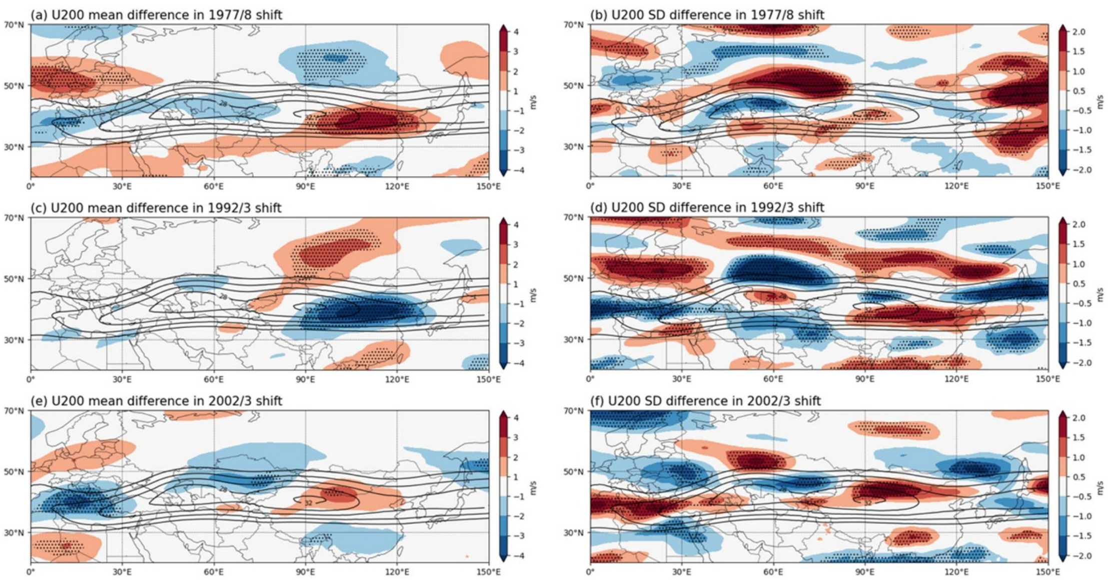

Figure 2. Examination of zonal wind at 200 hPa (U200) field change with respect to the mean state and interannual variance. (a) The shaded indicates the change of the U200 mean state difference between 1977/1978 shift. (b) Same with (a), except depicting the difference in the U200 standard deviation during the sub-periods. The contour lines show the climatology of U200 and the dotted region indicates where the difference exceeds 95% confidence levels. The middle panel (c) and (d) and the bottom panel (e) and (f) are the same with the upper panel (a) and (b) except they show the difference in 1992/1993 shift and the difference in 2002/2003 shift.

and prone to large fluctuations, with significant implications for weather predictability and extreme event occurrence across East Asia (Lin *et al* 2024).

Analysis of mean state changes associated with each detected regime shift reveals important difference in their characteristics and likely physical mechanisms (figure 2). The 1977/1978 and 1992/1993 shifts are characterized by clear jet strengthening and weakening, respectively (figures 2(a) and (c)). These are accompanied by slight meridional displacement of the jet axis (figure 1(c)). These patterns are entirely consistent with previous studies documenting decadal changes in the EAJ (Kwon *et al* 2007).

However, the newly identified 2002/2003 regime shift exhibits distinctly different characteristics. This shift shows a unique pattern characterized by simultaneous increases in both mean jet intensity and interannual variability (figures 2(e) and (f)). This finding aligns closely with recent work by Lin *et al* (2024). They reported a sharp increase in EAJ interannual variability since the end of the 20th century, providing independent confirmation of our results.

To rigorously assess the sensitivity and robustness of the newly detected 2002/2003 shift, we conduct comprehensive comparative analyses using multiple approaches. Sensitivity tests use alternative EAJ region definitions and comparisons across JRA-55 and 20CRv3 reanalysis datasets (see 'Methods'). Validation using CUSUM and Binary Segmentation algorithms (see 'Methods') confirms the consistency of regime shift timing across different datasets, region definitions, and detection methods (figure S1). This consistency provides strong evidence that the 2002/2003 transition represents a genuine physical regime shift in the EASM system rather than a statistical artifact.

3.2. From precipitation to land surface processes

Previous studies established that EAJ variability is primarily controlled by regional rainfall patterns over southern China through diabatic heating and upper-tropospheric circulation responses (figure S2(a); Kwon *et al* 2007, Wu *et al* 2010). The novel finding from our analysis is that this once-robust relationship shows different characteristics after 2003. Analysis of SST anomalies and velocity potential patterns at 200 hPa level (VP200) reveals fundamentally different tropical forcing between regime shifts (figure S4). The 1992/1993 shift shows Indian Ocean-to-Pacific propagation of upper-level divergence anomalies, while the 2002/2003 shift exhibits the opposite patterns, with Pacific-to-Indian Ocean propagation. Despite these contrasting forcing patterns, multiple gauge-based precipitation datasets (GPCP, CPC Unified, and APHRODITE) consistently show minimal precipitation changes over southern China during the 2002/2003 shift (figures S2(b) and S3). The limited precipitation response likely reflects offsetting

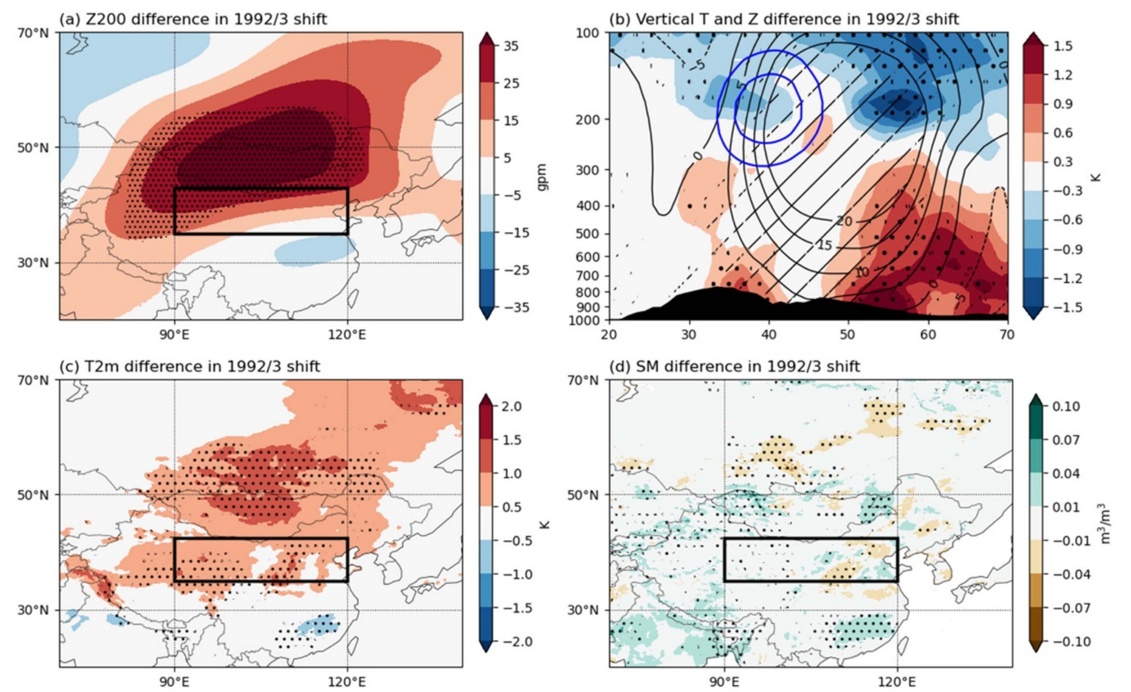

Figure 3. Examination of background variables of East Asian Jet and its vertical structure. The figures show the difference in 1992/1993 shift on (a) geopotential height over 200 hPa level (Z200), (b) the vertical structure of the atmosphere (shaded: T, black contours: Z) which is zonally averaged over East Asian longitude band (90°–120° E), (c) 2 m air temperature (T2m) and (d) soil moisture (SM) of which estimation range is from 0 to 289 cm depth. The dotted slashed region of each figure indicates where the difference exceeds 95% confidence levels conducted by bootstrap method and the black box covers where we defined as the East Asian Jet region. The blue contours in (b) show the climatology for zonal wind in 20 and 25 m s^{-1}.

changes in tropical cyclone characteristics: while TC frequency decreased in the 2000s (Ha and Zhong 2015), individual TC precipitation intensity increased (Shan and Yu 2021, Xu *et al* 2024), resulting in minimal net change in total TC-induced precipitation—a key component of southern China summer rainfall. The observed precipitation changes are insufficient to drive the jet intensification through the established diabatic heating mechanism. This indicates that other mechanisms beyond southern China precipitation may be driving recent EAJ mean changes.

Our analysis shows that the recent EAJ shift is more closely linked to East Asian land surface changes rather than precipitation-based mechanisms. Examination of atmospheric circulation patterns reveals distinct differences between the 1992/1993 and 2002/2003 regime shifts (figures 3 and 4).

The 1992/1993 shift features warming anomalies extending from the surface through the mid-troposphere, particularly pronounced north of the jet axis (figure 3(b)). This warming pattern suggests that surface-driven thermal forcing induces thermal expansion in the mid-troposphere, leading to anti-cyclonic circulation anomalies at 200 hPa (figure 3(a)) and contributing to EAJ weakening.

In contrast, the 2002/2003 shift feature significant positive geopotential height anomalies at 200 hPa centered over the Tibetan Plateau (figure 4(a)). The vertical structure, centered at approximately 150 hPa (figure 4(b)), indicates strengthening of the Tibetan Plateau High (TPH). The TPH plays a critical role in modulating the EASM system (Boos and Kuang 2010, Ha *et al* 2012) and influences both EAJ strength and position (Ding *et al* 2009, Wu *et al* 2010). The strengthening appears most prominent in the 80–100° E longitude band, corresponding to the Tibetan Plateau location (figure S5) and suggesting direct physical connection between plateau surface processes and upper-level circulation changes.

Land surface condition changes reveal important differences between the two regime shifts. The 1992/1993 shift was associated with substantial surface warming over Inner East Asia, north of the EAJ region (figure 3(c)). These finding align with previous studies indicating that warming in this region likely triggered the observed circulation changes (Dong *et al* 2016, Chang-yan *et al* 2020).

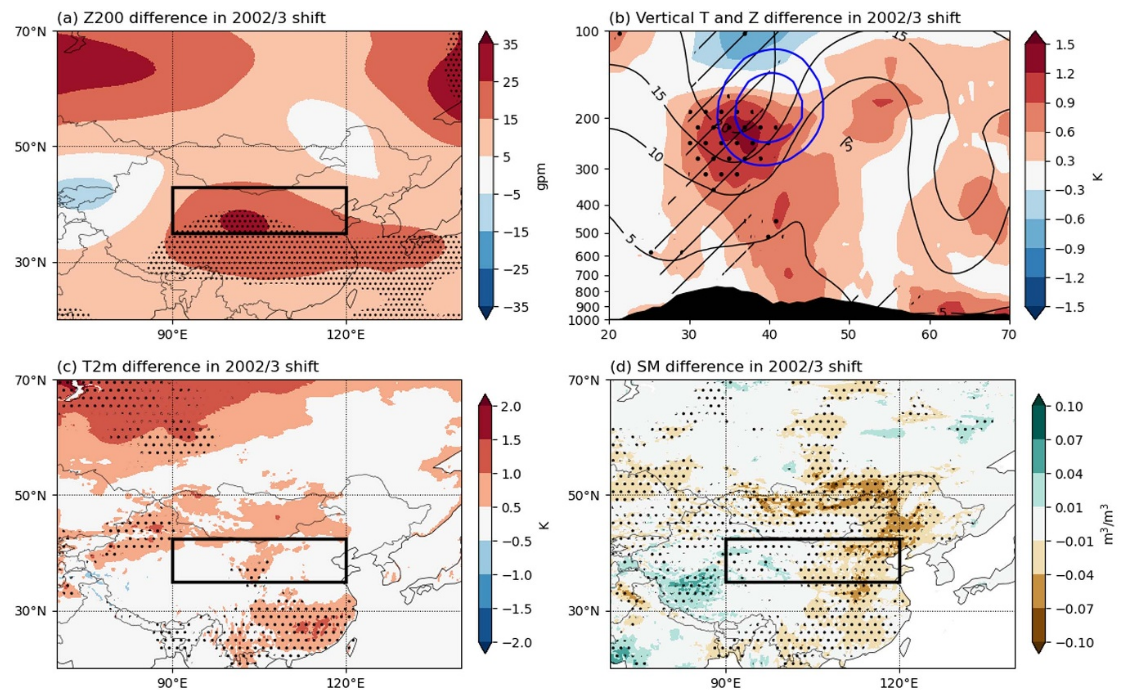

Figure 4. Same with figure 3, except showing the 2002/2003 shift.

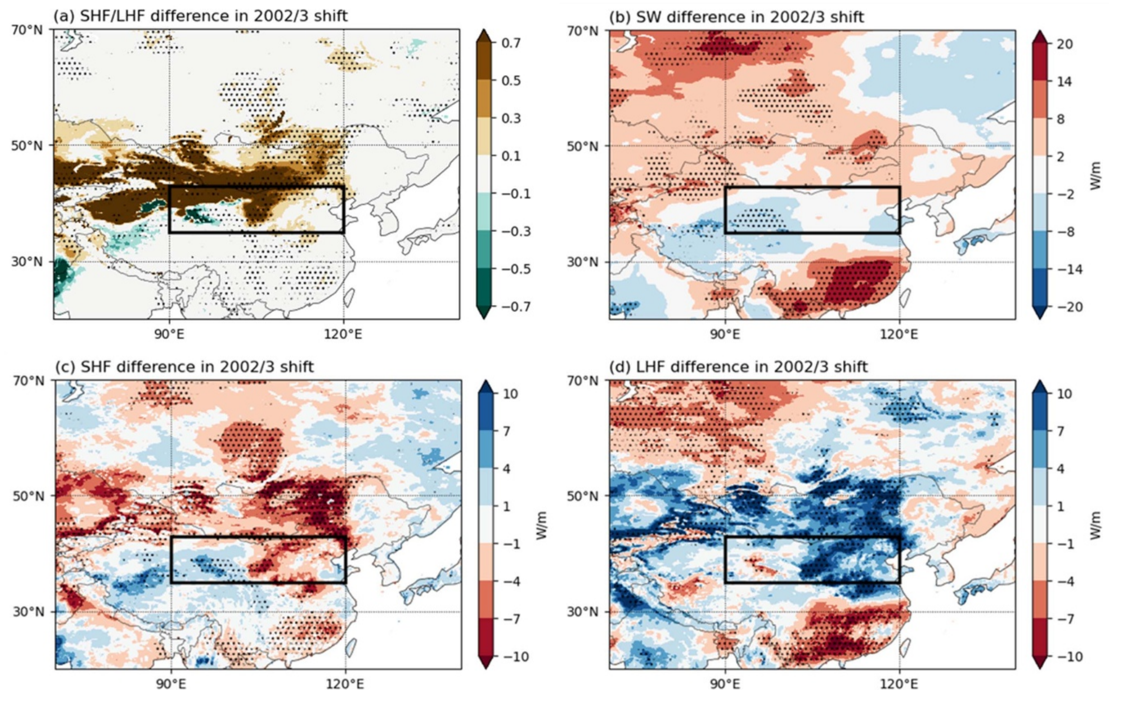

Figure 5. Examination of surface energy balance and radiation field in 2002/2003 shift. (a) The change in the Bowen ratio (SHF/LHF) representing the ratio of sensible heat flux to latent heat flux, (b) surface net shortwave radiation (SW), (c) surface sensible heat flux (SHF), and (d) surface latent heat flux (LHF). The dotted region indicates where the difference exceeds 95% confidence levels conducted by bootstrap method and the black box covers where we defined as the East Asian Jet region (EAJ; 90°–120° E, 35°–43° N).

The 2002/2003 period exhibits significant surface warming over southern China (figure 4(c)), generating a different spatial pattern of surface thermal forcing. This warming pattern is consistent with typical conditions during strong TPH seasons (Fan *et al* 2022, Tan *et al* 2023). Enhanced TPH conditions increase downward shortwave radiation at the surface (figure 5(b)) and raise sensible heat fluxes, resulting in anomalous surface heating across southern China (figure 5(c)).

The TPH strengthening during the 2002/2003 shift arises from synergistic local and remote forcings. Locally, box-averaged analysis over the Tibetan Plateau (80–100° E, 30–40° N) reveals significant enhanced convection (figure S6(a); $\Delta\omega300 = -0.0042$ Pa s^{-1}, $p < 0.01$) despite relatively weak spatial signals—likely reflecting data sparsity in this complex terrain (Yang *et al* 2020, Ma *et al* 2024). This enhanced ascent coincides with increased soil moisture and latent heat flux over northern plateau region (figures 4(d) and 5(d)), supporting localized diabatic heating (Luo *et al* 2024).

Remotely, the dominant forcing comes from western North Pacific, where SST warming drives enhanced tropical convection and upper-level divergence (figure S4(b)). This generates Rossby wave sources that maintain the TPH through remote dynamical forcing. Streamfunction budget analysis (see 'Methods') at 150 hPa reveals characteristic quadrature relationships: remote divergence of east of the plateau ridge supplies energy while local vorticity advection provides damping, establishing the stationary wave pattern (figures S6(b)–(d)). Taken together, these diagnostics delineate a coherent stationary wave maintenance mechanism by which combined local (Tibetan Plateau) and remote (western North Pacific) diabatic heating sustains the strengthened TPH.

3.3. Enhanced L–A coupling in the new regime

3.3.1. Transition to dry regime conditions and enhanced coupling variability

Another key feature of the 2002/2003 regime shift is pronounced and widespread drying across East Asia, notably stronger than during previous regime shifts (figure 4(d)). Change-point analysis of whole-column soil moisture reveals a significant transition in 2003, coincident with the EAJ shift (figure S7). This temporal alignment suggests that drying has extended into deeper soil layers, indicating a persistent shift in surface hydrological conditions.

In regions north of 30° N, documented soil moisture reduction is accompanied by reduced latent heat flux and increased sensible heat flux (figures 4(d) and 5(c), (d)). This systematic change in surface energy flux partitioning provides insights into hydrological regime transitions in the region. Following the soil moisture-regime framework (Hsu and Dirmeyer 2023), the observed changes suggest that Inner East Asia experienced a shift toward more frequent dry regime. In dry regime, soil moisture deficits become so severe that most available energy is partitioned into sensible heat flux, leading to maximum SM–T coupling strength as surface temperature becomes highly sensitive to soil moisture variations (see 'Methods').

The shift toward moisture-limited conditions is clearly evidenced by significant increases in the Bowen ratio field over Inner East Asia (figure 5(a)). This increase indicates that a greater proportion of available energy is partitioned into sensible heat flux rather than latent heat flux, reflecting reduced evapotranspiration capacity due to soil moisture constraints. The spatial pattern of Bowen ratio increases corresponds closely with regions experiencing the most pronounced soil moisture decline, providing clear evidence that Inner East Asia has shifted toward dry regime where moisture availability severely limits evapotranspiration.

Contrary to expectations based on surface changes (Zhang *et al* 2020), SM–T coupling mean state shows no significant change over Inner East Asia during the 2002/2003 shift, although there is a pronounced increase during the 1992/1993 shift (figure S8). Instead, coupling variability shows a notable increase after 2003 (figure 6(c)). This enhanced variability represents a different type of change in the L–A system that can be understood through the interaction between soil moisture conditions and atmospheric temperature advection patterns.

The substantial soil moisture decline since 2003 has fundamentally altered the thermal buffering capacity of the land surface. Under dry soil conditions, the coupling strength becomes highly sensitive to atmospheric conditions, particularly temperature advection patterns. When warm atmospheric conditions prevail, dry soils facilitate maximum coupling strength as most available energy is converted to sensible heat flux, rapidly warming the near-surface atmosphere. However, this mechanism can be offset by cold air advection, such as polar air mass invasions, In wet soil regions, enhanced atmospheric moisture content increases the effective heat capacity of the lower atmosphere, providing thermal buffering against rapid temperature drops. Conversely, in areas with severely reduced soil moisture, this thermal buffering is absent, resulting in more abrupt and intense cooling when cold air advection occurs (Seneviratne *et al* 2010). This phenomenon is analogous to the extreme diurnal temperature variations observed in desert regions, where the absence of moisture leads to rapid heating during the day and rapid cooling at night due to lack of thermal buffering.

This mechanism explains why mean coupling strength may not have shifted dramatically while variability increased substantially. As a result, Inner East Asia now experiences extreme variations in coupling strength that were not present when soil moisture provided thermal stability.

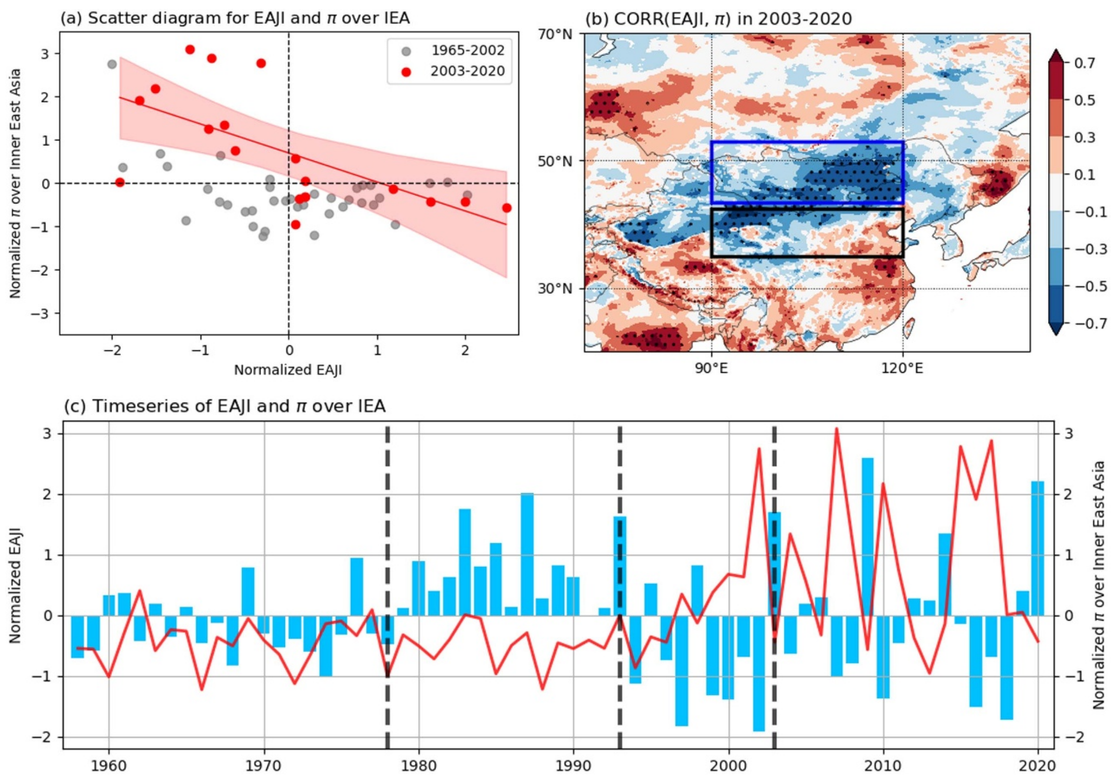

Figure 6. Relationship between the East Asian Jet index (EAJI) and the L–A coupling strength (π) over Inner East Asia (IEA) after 2002/3 shift. (a) Scatter diagram for normalized EAJI and normalized π averaged over IEA region during 1965–2002 period (gray dots) and 2003–2020 period (red dots). The red line indicates linear regression between two indices with shading as 95% confidence interval. The correlation coefficients between EAJI and π over IEA during pre-period and post-period are −0.357 and −0.652, respectively. (b) The spatial map of the correlation coefficient of EAJI timeseries on π field during 2003–2020 period. The black box covers the East Asian Jet region (EAJ; 90°–120° E, 35°–43° N) and the blue box covers the Inner East Asian region (IEA; 90°–120° E, 43°–53° N). The dotted area marks where its confidence levels exceeds 95%. (c) Long-term variability of East Asian Jet and the L–A coupling strength over Inner East Asia. Bars show the timeseries of EAJI and the vertical dashed lines indicate the regime shift years. The red line graph explains the normalized π area-averaged over IEA.

Table 1. Correlation coefficients between land–atmosphere coupling variables during each sub-period. The table shows correlations between (1) East Asian Jet index (EAJI) and L–A coupling strength (π) over Inner East Asia (IEA), (2) L–A coupling strength (π) and lower-tropospheric thickness (500–1000 hPa), and (3) L–A coupling strength (π) and Bowen ratio, all calculated over the Inner East Asia region (IEA; 90°–120° E, 43°–53° N) for each regime period. The superscript * indicates the 95% significance levels.

Period	1965–1977	1978–1992	1993–2002	2003–2020
π (over IEA) & EAJI	0.289	0.388	−0.035	−0.652*
π (over IEA) & $\text{Thickness}_{500\text{–}1000\ \text{hPa}}$	0.300	−0.261	−0.082	0.754*
π (over IEA) & Bowen ratio	−0.317	−0.129	0.334	0.594*

3.3.2. EAJ-coupling relationships and atmospheric linkages

Our analysis reveals a striking relationship between EAJ variability and L–A coupling strength over Inner East Asia (90–120° E, 43–53° N), where the most prominent drying occurred after 2002/2003 (figure 6). The scatter plot (figure 6(a)) shows clear separation between pre-2002 and post-2003 periods. The latter period exhibits substantially stronger negative correlation between EAJ variability and L–A coupling strength. The correlation coefficients for each period (table 1) indicate that this strong linkage represents a novel feature of the post-2003 climate regime that was absent in earlier decades.

To understand the physical mechanisms underlying the enhanced L–A coupling and its relationship with EAJ variability, we examine correlations between L–A coupling strength (π) and surface energy partitioning indicators across different periods. Analysis reveals that correlations between coupling strength and Bowen ratio are weak and insignificant during the pre-2003 periods (1965–1977, 1978–1992, 1993–2002), but become strong and significant in the post-2003 period (2003–2020) (table 1). This emergence of coupling-Bowen ratio relationship after 2003 indicates that the L–A system underwent fundamental changes, with surface energy partitioning becoming more consistently moisture-limited.

Several mechanisms likely contributed to weak coupling-surface energy relationships in the earlier periods. Large-scale atmospheric dynamics may have masked local boundary-layer feedbacks during the pre-2003 periods (Deser *et al* 2012). More importantly, the land surface was likely more consistently in wet regime conditions during earlier periods, where sufficient soil moisture allowed substantial latent heat flux, preventing the development of strong coupling-energy partitioning relationships.

The emergence of significant coupling-Bowen ratio relationship during the post-2003 period reflects the transition toward more frequent dry regime conditions documented in section 3.3.1. This coherent relationship between coupling strength and surface energy partitioning provides quantitative evidence for the enhanced sensitivity of the L–A system to soil moisture variations under the new hydrological regime.

To examine physical linkages between surface processes and atmospheric thermal structure, we analyze relationships between L–A coupling strength and lower-tropospheric thickness (500–1000 hPa), which indicates thermal expansion in the lower atmosphere. We specifically choose lower-tropospheric thickness to test whether SM–T coupling effects can extend beyond the boundary layer height, which is traditionally considered the upper limit of local L–A interactions. This analysis allows us to investigate whether surface coupling signals can influence atmospheric structure at levels that potentially connect to larger-scale circulation patterns. In the post-2003 period, coupling strength exhibits significant positive correlations with both Bowen ratio and lower-tropospheric thickness, while earlier periods show weaker relationships (table 1). These correlations provide evidence that when the L–A system operates in dry regime conditions characteristic of the post-2003 period, enhanced sensible heating from maximum energy partitioning contributes to thermal expansion of the lower troposphere through direct atmospheric column warming. This lower-tropospheric warming can potentially influence upper-level circulation features including the EAJ through modification of pressure gradient patterns and thermal wind relationships via hydrostatic adjustment processes.

Spatial correlation maps between EAJ variability and L–A coupling strength provide additional validation (figure 6(b)), showing significant negative correlations over Inner East Asia during the post-2003 period. Composite analysis reveals that this relationship is accompanied by notable anomalies in vertical atmospheric structure (figures S9(b) and (d)). Strong EAJ years correspond to enhanced invasion of cooler Arctic air masses, creating conditions that suppress L–A coupling through rapid cooling in areas with reduced thermal buffering capacity. Weak EAJ years are marked by anticyclonic circulation patterns that promote warm air mass dominance, enabling maximum SM–T coupling strength under the prevailing dry soil conditions. This atmospheric modulation of coupling strength explains the strong negative correlation between EAJ intensity and coupling variability, and appears highly associated with the observed increase in EAJ variability since 2003.

4. Conclusions

This study provides detailed diagnostic analysis of the marked 2002/2003 EASM regime shift, characterized by abrupt intensification of both the mean state and interannual variability of the EAJ. Through analysis of reanalysis datasets, we identify two key distinguishing features of this transition: strengthening of the TPH and enhanced SM–T coupling variability over Inner East Asia. Both features represent different manifestations of L–A coupling processes, highlighting the important role of surface-atmosphere interactions in this particular regime shift.

Our findings provides complementary insights to Lin *et al* (2024), which demonstrated Atlantic Ocean forcing as the primary driver of enhanced EAJ variability since the late 20th century. The key distinction lies our focus on L–A interactions as a potential modulating factor for jet behavior. We demonstrate the emergence of significant negative correlation between SM–T coupling strength and EAJ variability specifically after 2003, alongside strong correlations with surface energy partitioning and lower-tropospheric thermal structure. This suggests that regional land surface processes may complement established remote oceanic controls in modulating recent EASM behavior.

The transition toward more dry regime conditions after 2003, evidenced by significant increases in the Bowen ratio over Inner East Asia, has fundamental altered the thermal buffering capacity of the land surface. Under these conditions, coupling strength becomes highly sensitive to atmospheric temperature advection patterns, explaining the enhanced variability observed in both L–A coupling and EAJ intensity. The enhanced jet variability contributes to considerable changes in large-scale circulation patterns across East Asia and promotes more frequent and intense extreme weather events, including heatwaves, droughts, and heavy precipitation events, through increased atmospheric meandering and persistent circulation anomalies (Screen and Simmonds 2014, Trouet *et al* 2018, Lin *et al* 2024) that can extend far beyond the East Asian region.

However, establishing definitive causality faces fundamental limitations when based solely on observation analysis. Changes in L–A coupling and jet variability can influence each other over time scales shorter than our seasonal averaging resolution, potentially creating bidirectional interactions. Surface-derived anomalies may trigger changes in upper-level circulation, while upper-level changes can simultaneously modify surface energy balance and soil moisture patterns. Additionally, both systems may respond to common external forcing, potentially creating spurious correlations. Therefore, while our results demonstrate strong associations and suggest plausible physical connections, definitive causal relationships require further investigation through controlled modeling experiments (Koster *et al* 2016, Teng *et al* 2019, Martius *et al* 2021).

Several factors likely have a hand in this strengthening of coupling. Notably, CMIP6 projections do not show consistent soil moisture decline in this region (Leng *et al* 2015, Huang *et al* 2017b, Zhao and Dai 2022), with Inner East Asia identified as having large model uncertainties—likely due to inadequate representation of human water management, land-use changes, and regional aerosol forcing (Scanlon *et al* 2018, Qiao *et al* 2022, Jia *et al* 2023). However, tree-ring reconstructions reveal that the recent drying is unprecedented over the past 200–300 years, suggesting strong anthropogenic influence despite model limitation. Given that global warming increases atmospheric evaporative demand (VPD) across various regions (Yuan *et al* 2019, Fang *et al* 2022), anthropogenic warming likely contributes to Inner East Asian soil desiccation. Furthermore, the documented aerosol reduction over China since the mid-2000s have been linked to increased surface shortwave radiation through 'brightening' effects, enhancing both soil moisture decline and VPD increase (Shi *et al* 2021a, Sarangi *et al* 2022, Samset *et al* 2025), thereby preconditioning the land surface for stronger coupling. These mechanisms collectively provide a coherent physical framework explaining why L–A coupling variability increased substantially after 2003, even as mean coupling strength showed only modest changes. While establishing definitive causality from observations alone remains challenging, this enhanced coupling represents a novel feature of the post-2003 climate regime that warrants further investigation through controlled modeling experiments.

Data availability statement

The analyses use publicly available dataset (ERA5, ERA5-Land, JRA-55, 20CRv3, GPCP, CPC Unified, APHRODITE, ERSSTv5) cited in the references.

Acknowledgments

This research is funded by the National Research Foundation of Korea (NRF-2021R1A2C1011827, RS-2023-00283239 and RS-2025-02363044) and by the Korean Meteorological Agency under the Grant KMI2018-07010. HK is supported by the National Research Foundation (NRF) grant funded by the Korea Government(MSIT)(RS-2021-NR055516).

Author contributions

Jiyun Nam 0009-0003-9064-6656
Data curation (equal), Formal analysis (equal), Investigation (equal), Methodology (equal), Visualization (equal), Writing – original draft (equal)

Shih-Yu Simon Wang 0000-0003-2009-2275
Supervision (equal), Validation (equal), Writing – review & editing (equal)

Jee-Hoon Jeong 0000-0002-3358-3949
Conceptualization (equal), Writing – review & editing (equal)

Hyungjun Kim 0000-0003-1083-8416
Investigation (equal), Writing – review & editing (equal)

Jin-Ho Yoon 0000-0002-4939-8078
Conceptualization (equal), Funding acquisition (equal), Resources (equal), Supervision (equal), Validation (equal), Writing – review & editing (equal)

References

Adler R F *et al* 2003 The version-2 global precipitation climatology project (GPCP) monthly precipitation analysis (1979–present) *J. Hydrometeorol.* **4** 1147–67

Boos W R and Kuang Z 2010 Mechanisms of poleward propagating, intraseasonal convective anomalies in cloud system–resolving models *J. Atmos. Sci.* **67** 3673–91

Chang E, Yeh S, Hong S, Kim J, Wu R and Yoshimura K 2014 Study on the changes in the East Asian precipitation in the mid-1990s using a high-resolution global downscaled atmospheric data set *J. Geophys. Res. Atmos.* **119** 2279–93
Chang-yan Z, Li D, Qian R and Dong-mei D 2020 An interdecadal change of summer atmospheric circulation over Asian mid-high latitudes and associated effects *J. Tropical Meteorol.* **26** 363–76
Chen M, Shi W, Xie P, Silva V B S, Kousky V E, Wayne Higgins R and Janowiak J E 2008 Assessing objective techniques for gauge-based analyses of global daily precipitation *J. Geophys. Res. Atmos.* **113**
Chen T-C and Chen J-M 1990 On the maintenance of stationary eddies in terms of the streamfunction budget analysis *J. Atmos. Sci.* **47** 2818–24
Chen W and Lu R 2014 A decadal shift of summer surface air temperature over Northeast Asia around the mid-1990s *Adv. Atmos. Sci.* **31** 735–42
Deser C, Phillips A, Bourdette V and Teng H 2012 Uncertainty in climate change projections: the role of internal variability *Clim. Dyn.* **38** 527–46
Ding R, Ha K-J and Li J 2010 Interdecadal shift in the relationship between the East Asian summer monsoon and the tropical Indian Ocean *Clim. Dyn.* **34** 1059–71
Ding Y, Sun Y, Wang Z, Zhu Y and Song Y 2009 Inter-decadal variation of the summer precipitation in China and its association with decreasing Asian summer monsoon Part II: possible causes *Int. J. Climatol.* **29** 1926–44
Dong B, Sutton R T, Chen W, Liu X, Lu R and Sun Y 2016 Abrupt summer warming and changes in temperature extremes over Northeast Asia since the mid-1990s: drivers and physical processes *Adv. Atmos. Sci.* **33** 1005–23
Fan W, Hu Z, Ma W, Ma Y, Han C, Han X, Yang Y, Yu H, Fu C and Wu D 2022 Dominant modes of Tibetan Plateau summer surface sensible heating and associated atmospheric circulation anomalies *Remote Sens.* **14** 956
Fang Z, Zhang W, Brandt M, Abdi A M and Fensholt R 2022 Globally increasing atmospheric aridity over the 21st century *Earth's Future* **10** e2022EF003019
Ha K, Heo K, Lee S, Yun K and Jhun J 2012 Variability in the East Asian monsoon: a review *Meteorol. Appl.* **19** 200–15
Ha Y and Zhong Z 2015 Decadal change in tropical cyclone activity over the South China Sea around 2002/03 *J. Clim.* **28** 5935–51
Hersbach H *et al* 2019 Global reanalysis: goodbye ERA-Interim, hello ERA5 (available at: https://doi.org/10.21957/VF291HEHD7)
Herzschuh U *et al* 2019 Position and orientation of the westerly jet determined Holocene rainfall patterns in China *Nat. Commun.* **10** 2376
Hsu H and Dirmeyer P A 2023 Soil moisture-evaporation coupling shifts into new gears under increasing CO2 *Nat. Commun.* **14** 1162
Huang B, Thorne P W, Banzon V F, Boyer T, Chepurin G, Lawrimore J H, Menne M J, Smith T M, Vose R S and Zhang H-M 2017a Extended reconstructed sea surface temperature, version 5 (ERSSTv5): upgrades, validations, and intercomparisons *J. Clim.* **30** 8179–205
Huang G, Hu K and Xie S-P 2010 Strengthening of Tropical Indian Ocean teleconnection to the northwest Pacific since the mid-1970s: an atmospheric GCM study* *J. Clim.* **23** 5294–304
Huang J *et al* 2017b Dryland climate change: recent progress and challenges *Rev. Geophys.* **55** 719–78
Huang R, Chen J and Huang G 2007 Characteristics and variations of the East Asian monsoon system and its impacts on climate disasters in China *Adv. Atmos. Sci.* **24** 993–1023
Jia Q, Jia H, Li Y and Yin D 2023 Applicability of CMIP5 and CMIP6 models in China: reproducibility of historical simulation and uncertainty of future projection *J. Clim.* **36** 5809–24
Kim C-J, Qian W, Kang H-S and Lee D-K 2010 Interdecadal variability of East Asian summer monsoon precipitation over 220 years (1777–1997) *Adv. Atmos. Sci.* **27** 253–64
Kobayashi S *et al* 2015 The JRA-55 reanalysis: general specifications and basic characteristics *J. Meteorol. Soc. Japan II* **93** 5–48
Koster R D, Chang Y, Wang H and Schubert S D 2016 Impacts of local soil moisture anomalies on the atmospheric circulation and on remote surface meteorological fields during boreal summer: a comprehensive analysis over North America *J. Clim.* **29** 7345–64
Kwon M, Jhun J-G and Ha K-J 2007 Decadal change in east Asian summer monsoon circulation in the mid-1990s *Geophys. Res. Lett.* **34** L21706
Kwon M, Jhun J-G, Wang B, An S-I and Kug J-S 2005 Decadal change in relationship between east Asian and WNP summer monsoons *Geophys. Res. Lett.* **32**
Lee J-Y *et al* 2017 The long-term variability of Changma in the East Asian summer monsoon system: a review and revisit *Asia-Pac. J. Atmos. Sci.* **53** 257–72
Leng G, Tang Q and Rayburg S 2015 Climate change impacts on meteorological, agricultural and hydrological droughts in China *Glob. Planet Change* **126** 23–34
Lieting C and Renguang R 2000 Interannual and decadal variations of snow cover over Qinghai-Xizang Plateau and their relationships to summer monsoon rainfall in China *Adv. Atmos. Sci.* **17** 18–30
Lin L, Hu C, Wang B, Wu R, Wu Z, Yang S, Cai W, Li P, Xiong X and Chen D 2024 Atlantic origin of the increasing Asian westerly jet interannual variability *Nat. Commun.* **15** 2155
Lu R, Ye H and Jhun J-G 2011 Weakening of interannual variability in the summer East Asian upper-tropospheric westerly jet since the mid-1990s *Adv. Atmos. Sci.* **28** 1246–58
Luo H, Yu H, Hu Z, Zhou J, Zhang B, Yang Y, Cheng S, Gong Y and Ren Y 2024 Impact of the summer atmospheric heat source over the Tibetan Plateau on interannual variability of meridional circulation on the North side of the Tibetan Plateau *J. Clim.* **37** 3543–61
Ma Y *et al* 2024 Dataset of spatially extensive long-term quality-assured land–atmosphere interactions over the Tibetan Plateau *Earth Syst. Sci. Data* **16** 3017–43
Martius O, Wehrli K and Rohrer M 2021 Local and remote atmospheric responses to soil moisture anomalies in Australia *J. Clim.* **34** 1–48
Miralles D G, Van Den Berg M J, Teuling A J and De Jeu R A M 2012 Soil moisture-temperature coupling: a multiscale observational analysis *Geophys. Res. Lett.* **39** 2012GL053703
Muñoz-Sabater J *et al* 2021 ERA5-Land: a state-of-the-art global reanalysis dataset for land applications *Earth Syst. Sci. Data* **13** 4349–83
Page E S 1954 Continuous inspection schemes *Biometrika* **41** 100–15
Qiao L, Zuo Z and Xiao D 2022 Evaluation of soil moisture in CMIP6 simulations *J. Clim.* **35** 779–800
Rodell M, Famiglietti J S, Wiese D N, Reager J T, Beaudoing H K, Landerer F W and Lo M-H 2018 Emerging trends in global freshwater availability *Nature* **557** 651–9
Sampe T and Xie S-P 2010 Large-scale dynamics of the Meiyu-Baiu rainband: environmental forcing by the Westerly Jet* *J. Clim.* **23** 113–34

Samset B H *et al* 2025 East Asian aerosol cleanup has likely contributed to the recent acceleration in global warming *Commun. Earth Environ.* **6** 543

Sarangi C, Chakraborty T C, Tripathi S, Krishnan M, Morrison R, Evans J and Mercado L M 2022 Observations of aerosol–vapor pressure deficit–evaporative fraction coupling over India *Atmos. Chem. Phys.* **22** 3615–29

Scanlon B R *et al* 2018 Global models underestimate large decadal declining and rising water storage trends relative to GRACE satellite data *Proc. Natl Acad. Sci.* **115** E1080–9

Scott A J and Knott M 1974 A cluster analysis method for grouping means in the analysis of variance *Biometrics* **30** 507

Screen J A and Simmonds I 2014 Amplified mid-latitude planetary waves favour particular regional weather extremes *Nat. Clim. Change* **4** 704–9

Seneviratne S I, Corti T, Davin E L, Hirschi M, Jaeger E B, Lehner I, Orlowsky B and Teuling A J 2010 Investigating soil moisture–climate interactions in a changing climate: a review *Earth Sci. Rev.* **99** 125–61

Shan K and Yu X 2021 Variability of tropical cyclone landfalls in China *J. Clim.* **34** 9235–47

Shi H *et al* 2021a Surface brightening in eastern and central china since the implementation of the Clean Air Action in 2013: causes and implications *Geophys. Res. Lett.* **48** e2020GL091105

Shi P *et al* 2021b Significant land contributions to interannual predictability of East Asian summer monsoon rainfall *Earth's Future* **9** e2020EF001762

Slivinski L C *et al* 2019 Towards a more reliable historical reanalysis: improvements for version 3 of the Twentieth Century Reanalysis system *Q. J. R. Meteorol. Soc.* **145** 2876–908

Tan Z, Liu Y, Shao T, Luo R, Luo M and Xie Y 2023 Association between Tibetan heat sources and heat waves in China *J. Clim.* **36** 7905–24

Tao F, Zhang Z, Xiao D, Zhang S, Rötter R P, Shi W, Liu Y, Wang M, Liu F and Zhang H 2014 Responses of wheat growth and yield to climate change in different climate zones of China, 1981–2009 *Agric. For. Meteorol.* **189–190** 91–104

Teng H, Branstator G, Tawfik A B and Callaghan P 2019 Circumglobal response to prescribed soil moisture over North America *J. Clim.* **32** 4525–45

Trouet V, Babst F and Meko M 2018 Recent enhanced high-summer North Atlantic Jet variability emerges from three-century context *Nat. Commun.* **9** 180

Truong C, Oudre L and Vayatis N 2020 Selective review of offline change point detection methods *Signal Process.* **167** 107299

Wang X, Zhou W, Wang D and Wang C 2013 The impacts of the summer Asian Jet Stream biases on surface air temperature in mid-eastern China in IPCC AR4 models: SUMMER ASIAN JET STREAM AND ITS EFFECT ON TEMPERATURE IN MID-EASTERN CHINA *Int. J. Climatol.* **33** 265–76

Wu R, Wen Z, Yang S and Li Y 2010 An interdecadal change in southern China summer rainfall around 1992/93 *J. Clim.* **23** 2389–403

Xu M, Tan Y, Shi C, Xing Y, Shang M, Wu J, Yang Y, Du J and Bai L 2024 Spatiotemporal patterns of typhoon-induced extreme precipitation in Hainan Island, China, 2000–2020, using satellite-derived precipitation data *Atmosphere* **15** 891

Yang Z-L, Zhao L, He Y and Wang B 2020 Perspectives for Tibetan Plateau data assimilation *Natl Sci. Rev.* **7** 495–9

Yatagai A, Kamiguchi K, Arakawa O, Hamada A, Yasutomi N and Kitoh A 2012 APHRODITE: constructing a long-term daily gridded precipitation dataset for Asia based on a dense network of rain gauges *Bull. Am. Meteorol. Soc.* **93** 1401–15

Yim S-Y, Jhun J-G and Yeh S-W 2008 Decadal change in the relationship between east Asian–western North Pacific summer monsoons and ENSO in the mid-1990s *Geophys. Res. Lett.* **35** L20711

Yuan W *et al* 2019 Increased atmospheric vapor pressure deficit reduces global vegetation growth *Sci. Adv.* **5** eaax1396

Zhang P, Jeong J-H, Yoon J-H, Kim H, Wang S-Y S, Linderholm H W, Fang K, Wu X and Chen D 2020 Abrupt shift to hotter and drier climate over inner East Asia beyond the tipping point *Science* **370** 1095–9

Zhang Y, Kuang X, Guo W and Zhou T 2006 Seasonal evolution of the upper-tropospheric westerly jet core over East Asia *Geophys. Res. Lett.* **33** 2006GL026377

Zhao T and Dai A 2022 CMIP6 model-projected hydroclimatic and drought changes and their causes in the twenty-first century *J. Clim.* **35** 897–921

Zhou T *et al* 2009 Why the western Pacific subtropical high has extended westward since the late 1970s *J. Clim.* **22** 2199–215